

# Resistance effects due to magnetic guiding orbits

J. Reijniers and F. M. Peeters\*

*Departement Natuurkunde, Universiteit Antwerpen (UIA), Universiteitsplein 1, B-2610 Antwerpen, Belgium*

(October 24, 2018)

The Hall and magnetoresistance of a two dimensional electron gas subjected to a magnetic field barrier parallel to the current direction is studied as function of the applied perpendicular magnetic field. The recent experimental results of Nogaret *et al.* [Phys. Rev. Lett. **84**, 2231 (2000)] for the magneto- and Hall resistance are explained using a semi-classical theory based on the Landauer-Büttiker formula. The observed positive magnetoresistance peak is explained as due to a competition between a decrease of the number of conducting channels as a result of the growing magnetic field, from the fringe field of the ferromagnetic stripe as it becomes magnetized, and the disappearance of snake orbits and the subsequent appearance of cycloidlike orbits.

73.50.Jt; 73.50-h; 73.23

## I. INTRODUCTION

Recently, there has been a growing experimental and theoretical activity directed towards an increased functionality of present day electronic devices. Previously, electrical potentials were used to modify the current, while more recently one became interested in the effects of magnetic field profiles, modulated or not, on the motion of electrons in semiconductor structures. The latter is usually a heterostructure which contains a two-dimensional electron gas (2DEG). Inhomogeneous magnetic field profiles in the 2DEG are created by depositing superconducting or ferromagnetic materials on top of the heterostructure which is then patterned in the desired shape using modern nanolithography.<sup>1</sup>

These hybrid systems are important from a theoretical and technological point of view, since they open the door to new physics which might result in e.g. new magneto-electronic devices.<sup>2</sup> An example of such a new device is the Hybrid Hall effect device<sup>3,4</sup> in which the magnetic material provides a local magnetic field which influences locally the electron transport in the underlying 2DEG. The 2DEG then acts as a detector<sup>5</sup> measuring the magnetic state of the magnetic material.

The fringe field arising from a magnetic stripe forms a magnetic barrier for the electron motion in the 2DEG.<sup>6-11</sup> Barriers can be created in which the sign of the magnetic field alters in different regions of space. Due to this magnetic gradient, electrons can be bound at the boundary line between two regions of opposite magnetic field. The spectrum and the corresponding magnetic edge states have been studied recently.<sup>6,12-16</sup>

When an (1D) inhomogeneous magnetic field is applied across a quasi 1D wire, these magnetic edge states are confined electrically due to the wire confinement potential and they mix with the ordinary edge states.<sup>17</sup> Such a situation was recently realized by Nogaret *et al.*,<sup>18</sup> where the inhomogeneous magnetic profile was arising from a perpendicularly magnetized ferromagnetic stripe grown on top of the 2DEG. They measured the magneto- and Hall resistance as function of a background magnetic field, and observed a sharp resistance resonance effect, which they attributed to the formation and subsequent killing of magnetic edge states.

In the present work we give a detailed theoretical analysis of this experiment, using a semi-classical approach in which we consider the electrical and magnetic confinement quantum mechanically, and include scattering processes using classical arguments. Both, the measured Hall resistance and the magnetoresistance will be explained. We will show that the theoretical picture of Nogaret *et al.* only captures part of the physics which is involved and is unable to predict the correct position of the peak in the magnetoresistance and the Hall resistance.

The side and top view of the experimental setup of Nogaret *et al.*<sup>18</sup> are shown in Fig. 1. A Hall device consisting of a  $W = 2\mu\text{m}$  wide 2DEG channel in a GaAs/AlGaAs-heterojunction was fabricated, with electron density  $n_e = 1.94 \times 10^{15}\text{m}^{-2}$  and mean free path  $\ell = 4.5\mu\text{m}$  at 4.5K. A narrow ( $W_f = 0.5\mu\text{m}$ )  $32\mu\text{m}$  long ferromagnetic (Fe or Ni) stripe (thickness  $d_f = 200\mu\text{m}$ ) was grown a distance  $h = 80\text{nm}$  above the center of the electron channel.

The electron transport in the 2DEG is only influenced by the perpendicular component of the magnetic stray field. In absence of any background magnetic field the ferromagnetic stripe is magnetized along the easy axis, i.e. the  $y$ -direction, and the fringe field is situated outside the quasi 1D wire, i.e. in reservoir 1 and 2. Application of a perpendicular background magnetic field rotates the magnetization to align with the  $z$ -axis, and this will result in a stray field in the wire, which imposes a step magnetic field profile along the  $y$ -direction (see Fig. 1(b)). The actual magnetic field profile is slightly rounded (see Ref. 18) but we checked that our results are not influenced by this simplification. This magnetic step adds an inhomogeneous magnetic field component to the uniform applied magnetic field  $B_a$  which induces the observed resistance effects. In the present analysis, we restrict ourselves to a Fe-stripe (saturation magnetization: 1.74 T), since this was studied most thoroughly

in Ref. 18 and produced the most pronounced resonance effect.

This paper is organized as follows. In Sec. II we present our theoretical approach. In Sect. III we calculate the two terminal resistance as function of the applied background magnetic field. The Hall resistance is studied in Sect. IV and in Sect. V the magnetoresistance is calculated. We will discuss differences between our theoretical results and the experimental (and theoretical) results of Nogaret *et al.*<sup>18</sup> Our theoretical explanation for the observed resonance effect in the magnetoresistance deviates from the one proposed in Ref. 18. In Sect. VI we summarize our conclusions.

## II. THEORETICAL APPROACH

The magneto- and Hall resistance are measured experimentally by use of a *four-terminal* configuration. In contrast to the theoretical study of Nogaret *et al.*<sup>18</sup>, we will retain this feature in the present discussion. The four-terminal configuration is schematically shown in Fig. 2 for (a) a Hall measurement and (b) a magnetoresistance measurement. The leads are in thermodynamical equilibrium and can be characterized by a chemical potential  $\mu_i$ . Each reservoir injects a current  $I_i$  of electrons into the 1D wire. If several bands are occupied, we have to consider a many-channel situation, and according to Büttiker,<sup>19</sup> the current in each of the leads is given by

$$I_i = \frac{e}{h} \sum_{n,n'} \left\{ [\delta_{n,n'} - T_{ii}(n, n')] \mu_i - \sum_{j \neq i} T_{ij}(n, n') \mu_j \right\}, \quad (1)$$

where  $T_{ij}(n, n')$  is the probability for an electron in channel  $n$  of lead  $i$  to be scattered/transmitted to  $n'$  of lead  $j$ . Current conservation requires  $N_i = R_{ii} + \sum_{j \neq i} T_{ij}$  for all  $i$ , with  $T_{ij} = \sum_{n,n'} T_{ij}(n, n')$  and  $R_{ii} = 1 - T_{ii}$  and  $N_i$  is the number of channels in lead  $i$ .

Each channel  $n$  contributes a probability  $T_{ij}(n)$  to the conductivity which is transmitted from probe 1 to probe 2. The total transmission from probe  $i$  to  $j$  then equals  $T_{ij} = \sum_{n \leq N} T_{ij}(n)$ , and Eq. (1) is simplified to

$$I_i = \frac{e}{h} \sum_n \left\{ [1 - R_{ii}(n)] \mu_i - \sum_{j \neq i} T_{ij}(n) \mu_j \right\}. \quad (2)$$

In this type of measurement, only two probes are current carrying, i.e.,  $i = 1, 2$ , which results in the condition  $I_1 = -I_2 = I$  while the other probes are voltage probes and do not carry any net current:  $I_3 = I_4 = I_5 = 0$ .

In order to calculate the four-terminal magneto- and Hall resistance, we will make another simplifying assumption that the voltage probes are weakly coupled, i.e. their influence on the net current  $I$  is very small

( $I = (\mu_1 - \mu_2)/R_{12,12}$ ) and the chemical potentials in each of the voltage probes can be calculated in the absence of the other voltage probes ( $\mu_i = (T_{i1}\mu_1 + T_{i2}\mu_2)/(T_{i1} + T_{i2})$  with  $i = 3, 4$ ). The general formula for this kind of resistance measurement is then readily obtained and given by

$$\begin{aligned} R_{12,3i} &= \frac{\mu_3 - \mu_i}{eI} = \frac{h}{e^2} \frac{1}{T_{12}} \frac{T_{31}T_{i2} - T_{32}T_{i1}}{(T_{31} + T_{32})(T_{i1} + T_{i2})} \\ &= \frac{h}{e^2} \frac{1}{T_{12}} F = R_{12,12} F, \end{aligned}$$

which is the two terminal resistance  $R_{12,12}$  multiplied with a geometrical form factor  $F$ , which is less than one.

In the following we will first calculate the two-terminal resistance  $R_{12,12}$  and then concentrate on the geometrical form factor  $F$  in the case of a Hall or magnetoresistance measurement.

## III. THE ENERGY SPECTRUM AND THE TWO-TERMINAL RESISTANCE

The two-terminal resistance is given by  $R_{12,12} = (\mu_2 - \mu_1)/I$ . We know that in the absence of any collisions, the current which flows from reservoir 1 to 2 is determined by the number of subbands  $N$  which are occupied at the Fermi level. Since the mean free path in the experiment of Nogaret *et al.*<sup>18</sup> is  $\ell = 4\mu\text{m}$ , which is larger than the wire width ( $W = 2\mu\text{m}$ ), we can, to a good approximation, neglect the influence of scatterers on the spectrum and calculate the number of channels quantum mechanically following the work of Müller<sup>12</sup> for a pure quasi 1D quantum wire.

We consider a system of noninteracting electrons moving in the  $xy$ -plane subjected to a hard wall confinement  $-W/2 < x < W/2$ , where  $W$  is the width of the wire. The electrons are subjected to a magnetic field profile  $\vec{B} = (0, 0, B_z(x))$ . This profile equals  $B_z = B_i(B_a) + B_a$ , where  $B_a$  is the uniform applied background field and  $B_i$  is the induced magnetic field profile due to the magnetized stripe.

In correspondence with Ref. 18 we will model the shape of the induced magnetic field profile by the average magnetic field on the respective sides of the magnetic stripe edges, i.e. at saturation the magnetic field profile is given by  $B_{sat} = B_1 - (B_1 + B_2)\theta(|x| - W_f/2)$ , where  $\theta$  is the heavyside step function and  $B_1 = -0.06$  Tesla and  $B_2 = 0.28$  Tesla are the modeled magnetic field strengths underneath and away from the stripe as shown in Fig. 1(c). We also performed the calculations for the exact magnetic field profile, but this resulted in negligible small quantitative differences.

We model the magnetization of the stripe by considering two limiting cases: (A) when the stripe is already magnetized at  $B_a = 0$  Tesla (as was considered by Nogaret *et al.*), i.e.  $B_i = B_{sat} \text{sign}(B_a)$  which is the hard magnet case, and (B) when the applied

magnetic field magnetizes the stripe as for soft magnets. In case (B) we assume  $B_i$  to be linearly varying with applied background magnetic field  $B_a$ , up to  $B_a = 0.05$  Tesla, where saturation is attained according to Ref. 18. The induced magnetic field is then given by  $B_i = B_{sat}\{1 - [1 - \theta(|B_a| - 0.05)](1 - |B_a|/0.05)\}$ . The actual experimental behaviour is expected to be situated closer to situation (B) than to (A).

The one-particle states are described by the Hamiltonian

$$H = \frac{1}{2m_e} p_x^2 + \frac{1}{2m_e} \left[ p_y - \frac{e}{c} A(x) \right]^2 + V(x), \quad (3)$$

where  $V(-W/2 < x < W/2) = 0$  and  $V(x < -W/2) = V(x > W/2) = \infty$ . Taking the vector potential in the Landau gauge  $\vec{A} = (0, A_y(x), 0)$ , such that  $\partial A_y(x)/\partial x = B_z(x)$ , we arrive at the following 2D Schrödinger equation

$$\left\{ \frac{\partial^2}{\partial x^2} + \left[ \frac{\partial}{\partial y} + A_y(x) \right]^2 + 2[E - V(x)] \right\} \psi(x, y) = 0, \quad (4)$$

where the magnetic field is expressed in  $B_0$ , magnetic units are used for a homogeneous field of  $B_0 = 1$  Tesla, i.e., all lengths are measured in  $l_0 = \sqrt{\hbar c/eB_0} = 0.0257 \mu\text{m}$  and energy is measured in units of  $E_0 = \hbar e B_0/m_e c = 1.7279 \text{meV}$ .  $H$  and  $p_y$  commute due to the particular choice of the gauge, and consequently the wavefunction becomes

$$\psi(x, y) = \frac{1}{\sqrt{(2\pi)}} e^{-iky} \phi_{n,k}(x), \quad (5)$$

which reduces the problem to the solution of the 1D Schrödinger equation

$$\left[ -\frac{1}{2} \frac{d^2}{dx^2} + V_k(x) \right] \phi_{n,k}(x) = E_{n,k} \phi_{n,k}(x), \quad (6)$$

where it is the  $k$ -dependent effective potential

$$V_k(x) = \frac{1}{2} [x B_z(x) + k]^2 + V(x), \quad (7)$$

which contains the two dimensionality of the problem.<sup>6</sup> We solve Eq. (6) numerically by use of a discretization procedure.

For given applied background magnetic field we calculated the energy spectrum for case (A) with  $W = 2\mu\text{m}$ . The results are shown in Fig. 3 for  $B_a/B_0 = 0; 0.1; 0.5$ . These energy spectra are symmetric in  $k$  and for small  $B_a$  consist of the superposition of two parabolic spectra. For small  $k$ -values and for energies below the intersection of the two parabolas Landau levels are present due to electrons which are bound underneath the stripe. These levels shift away from each other as the background magnetic field increases, due to the increase of the magnetic

field underneath the stripe ( $B_1$ ). For increasing magnetic field the two parabolas shift further away from each other, towards higher  $|k|$  values. Due to the confinement of the wire, each parabola is infinitely duplicated, where its maximum is shifted to higher energy and to lower  $k$ -values. For higher magnetic fields ( $B_a > 0.5B_0$ ) Landau levels arise, due to the magnetic field away from the stripe ( $B_2 < B_1$ ) which is now strong enough to localize electrons into cyclotron orbits.

The classical trajectories (for  $E = 4E_0$ ) corresponding to the different regions in  $k$ -space are shown on top of Fig. 3. We restricted ourselves to trajectories of states at energy  $E = 4E_0$ , since at zero temperature only channels with energy  $E = \epsilon_F = 4E_0 = 6.9 \text{meV}$  contribute to the conductivity.

For (B) the spectrum at  $B_a/B_0 = 0; 0.03; 0.06$  and the corresponding classical orbits at the Fermi energy are shown in Fig. 4. For  $B_a = 0$  the magnetic stripe is not magnetized and the spectrum consists only of the potential confined levels. One single parabola (and its duplicates due to confinement) centered around  $k = 0$  is found which splits into two and its center shifts towards higher  $|k|$ -values. Below the intersection of the two shifted parabolas Landau states are formed. Notice that some levels intersect the Fermi energy twice as much as before. These Landau states separate further away from each other for increasing magnetic field. For  $B_a \geq 0.05B_0$  the spectra are identical to the ones of (A).

The number of conducting channels is given by the number of energy levels intersecting the Fermi energy  $N$ , and hence the current is

$$I = \frac{e}{h} T_{12}(\mu_i - \mu_j) \quad (8)$$

with  $T_{12} = \sum_{n < N} T_{12}(n) = N$ , since in absence of any collisions  $T_{12}(n) = 1$ .

Nevertheless, the mean free path measured by Nogaret *et al.* is smaller than the length of the wire  $L_y = 16 \mu\text{m}$  and also smaller than the distance between the probes. Thus, scattering will play an important role in electron transport and consequently  $T_{12}(n)$  will be less than 1. In order to account for this, we will estimate the transmission coefficient for every channel using classical arguments. Since we consider the voltage probes as weakly coupled, they result in a very weak perturbation of the electron-current path, and scattering due to the voltage probes will be neglected. The only scattering we consider is due to collisions with impurities and other imperfections in the 1D-channel.

The rate at which these collisions occur depends classically on the velocity in the  $y$ -direction, the length of the wire and the scattering time. The lower the velocity in the  $y$ -direction, the longer it takes to overcome the distance between probe 1 and probe 2, and the more probable it will be to experience a scattering event. Because of this we consider the transmission probability of every channel to be proportional to its velocity

$v_y = -\partial E_n(k)/\partial k|_{\epsilon_F}$  and the scattering time  $\tau$ , and inversely proportional to the length  $L_y$  of the wire, i.e.,

$$T_{12}(n) \sim \frac{v_y(n)\tau}{L_y}. \quad (9)$$

So finally, we arrive at the two terminal resistance

$$R_{12,12} = \frac{1}{\alpha} \frac{\hbar}{e^2} \frac{1}{\sum_n v_y(n)}, \quad (10)$$

where  $n$  runs over all the  $N$  electron states with positive velocity (or negative velocity) at the Fermi energy  $\epsilon_F$ , and  $\alpha$  is a function of  $L_y$  and  $\tau$ .

First we will discuss the change of the two-terminal resistance  $R_{12,12}$  with respect to the situation in absence of the ferromagnetic stripe  $R_{12,12}^0$ , which we will call the *induced* resistance  $R_{12,12}/R_{12,12}^0$ . This property was also calculated and discussed by Nogaret *et al.*,<sup>18</sup> and is plotted in Fig. 5 as function of the applied magnetic field  $B_a$  for the approach of Ref. 18 (dashed curve) and ours (dotted and solid curves). The zero temperature result is shown in the inset.

We notice that at zero temperature, many discontinuous jumps are present. As we will see further on, their position is very sensitive to the Fermi-energy and they disappear at 4.2 K. The energy distribution function  $f(E, T) = \{\exp[(E - \epsilon_F)/k_B T] + 1\}^{-1}$  is not a stepfunction for nonzero temperature and consequently also electrons with energy different from  $\epsilon_F$  will contribute to the conductivity. This will smoothen out these oscillations, as is shown in Fig. 5. Also the broadening of the energy levels due to e.g. potential fluctuations will have such a smoothening effect on the resistance curves. Hence, we will only show these smooth curves in the next figures.

The curves (A) and (B) differ only for  $B_a < 0.05B_0$ . In case (A) the resistance for  $B_a = 0$  is larger than in the absence of the magnetic stripe. Increasing the background magnetic field results in a slight overall increase of the induced resistance. At  $B_a = 0.02B_0$  the induced resistance reaches its maximum, then it decreases rapidly.

The induced resistance in case (B) starts at 1 for  $B_a = 0$ , increases more rapidly and attains its maximum at a slightly higher  $B_a$ -value, i.e.,  $B_a = 0.0375B_0$ . Then it decreases rapidly up to  $B_a = 0.2B_0$ . We again notice oscillations at zero temperature (see inset), but fewer than for case (A). For larger  $B_a$ -values the oscillations disappear and the scaled resistance increases ultimately to one.

Nogaret *et al.*<sup>18</sup> obtained theoretically a somewhat similar behaviour, as is indicated by the dashed curve, except for the peak which was situated at a slightly higher value  $B_a = 0.06B_0$ . They made the assumption that the stripe was already fully magnetized at  $B_a = 0$  like in our case (A). Moreover they considered the magnetoresistance for a homogeneous magnetic field profile with magnetic field strength  $B_a$ , and considered the effect of the magnetic stripe profile by adding classical trajectories of states which arise due to the presence of the stripe.

In order to simplify the problem, they only considered states which do not reach (classically) the edge of the sample. They attributed the initial positive magnetoresistance to *snake orbits* (see situation “o” in Fig. 3(a)) which are killed with increasing magnetic field and therefore no longer contribute to the conductivity for larger fields. At  $B_a = 0.06B_0$  all snake orbits have vanished and it is due to this, they inferred, that the resistance reaches its maximum. However if the magnetic field is larger than  $0.06B_0$ , the magnetic field has the same sign over the whole sample but has different strength under the stripe and away from it, and a new type of magnetic edge states, so called *cycloidlike* states (see the states indicated by “◁” in Fig. 3(b)), arises, which again enhances conductivity and thus lowers the resistance. The fact that the influence of the latter orbits vanishes for larger  $B_a$ -values is due to the decrease of the velocity of these states with decreasing relative difference between the two neighboring magnetic fields.

In case (A), when the saturation magnetization is already attained at  $B_a = 0$ , we cannot attribute the existence of the (small) peak to the creation or annihilation of a certain classical state. Fig. 3 shows the energy spectrum and the corresponding classical states at the Fermi-energy  $\epsilon_F = 4E_0$  for (a)  $B_a = 0$ , (b)  $B_a = 0.1B_0$  and (c)  $B_a = 0.5B_0$ . From this figure we see that the enhancement of the resistance is a pure quantum mechanical effect and involves many different types of states with different velocities. Therefore an explanation based on the appearance or disappearance of only snake orbits as done by Nogaret *et al.* is not possible, at least for small  $B_a$ . The discontinuous behaviour for small  $B_a$  (see the inset in Fig. 5) is due to edge states at the Fermi-level whose energy moves through the Fermi level and then no longer contribute to the conduction. They have nonzero velocity and hence this is also reflected in the resistance. For larger  $B_a > 0.05B_0$  the curve coincides with the one of case (B).

In case (B), the initial magnetoresistance can be understood more easily. For  $B_a = 0$ , the stripe is not yet magnetized and thus there is no effect of the magnetic stripe. Fig. 4(a) shows subbands formed due to the quasi 1D confinement ( $N = 70$  subbands contribute to the conduction). Already for a small applied magnetic field, a relative large magnetic field is induced in the wire due to the magnetization of the ferromagnetic stripe. Whereas, for  $B_a = 0$  the only confinement was due to the edges of the sample, the magnetic field tends to localize electrons into cyclotron orbits and thus forces them in Landau levels, which separate further in energy with increasing magnetic field. As a consequence less channels will intersect the Fermi-level and consequently less channels contribute to electron transport and the resistance increases.

But there is a competing effect due to the presence of the magnetic stripe which tends to lower the induced resistance: new edge states arise (see the states indicated by “▷” and “◁” in Figs. 3 and 4) which travel in the opposite direction of the normal edge states. In terms

of energy spectra, this effect is contained in subbands which contribute twice to the conductivity, as can be seen in Figs. 3(b,c). It overcomes the previous one at  $B_a = 0.0375B_0$ , and the induced resistance decreases. This effect contributes even for  $B_a > 0.06B_0$ , when the magnetic field has the same sign in the whole wire, and the previously mentioned cycloidlike orbits appear. For increasing magnetic field their influence decreases, although their number with respect to normal edge states increases. This is due to their velocity, which decreases for increasing  $B_a$  for reasons given by Nogaret *et al.*

In the following sections, we will try to reproduce the experimental results obtained by Nogaret *et al.* First we will concentrate on the Hall resistance, before we focus on the magnetoresistance.

#### IV. THE HALL RESISTANCE

In order to calculate the magneto- and Hall resistance we will further simplify the problem, by making the assumption of symmetrical probes. In case of the Hall resistance, the two voltage probes, i.e. probe 3 and 4, are in front of each other as is clear from Fig. 2, and due to this symmetry the transmission probabilities can be written as  $T_{31} = T_{42} = T$  and  $T_{32} = T_{41} = t$ . The Hall resistance then attains a very simple form

$$R_{12,34} = \frac{1}{\alpha} \frac{\hbar}{e^2} \frac{1}{T_{12}} \frac{(T/t - 1)}{(T/t + 1)}, \quad (11)$$

as was already derived in Ref. 20. Note that there is additionally one parameter  $\alpha$  and one function  $t/T$  which describe the behaviour of the Hall resistance. In the absence of any magnetic field  $t/T = 1$ , and consequently the Hall resistance reduces to zero. As the cyclotron radius decreases, electrons will be localized closer to the edge (in edge states) and consequently the probability for an electron *bouncing* on one edge to be transmitted in a probe on the other side of the wire decreases drastically, i.e. exponentially, with increasing magnetic field, as can be inferred from Ref. 20. Consequently  $t/T$  will decrease rapidly and ultimately for already a small applied magnetic field the geometrical form factor  $F = (T/t - 1) / (T/t + 1)$  will be 1 in which case the Hall resistance equals the two-terminal resistance  $R_{12,12}$ .

In order to obtain qualitative agreement with experiment, we follow Ref. 21 and take the following functional form for  $t/T = \exp[-25B_a - (35B_a)^2]$  with  $B_a$  expressed in Tesla. If we take  $R_{12,34}^0(B_a) = (3669.4 * B_a)\Omega$  as the functional form of the Hall resistance in absence of the magnetic stripe, which we obtained from a linear fit of the experimental result by Nogaret *et al.*, we obtain the induced Hall resistance  $R_{12,34}/R_{12,34}^0$  as shown in Fig. 6 for case (A) and (B) (dotted and solid curves, respectively) which is compared with the experimental result (dashed curve).

We notice that the induced Hall resistance for  $B_a = 0$  approaches 0.5 in both cases (A) and (B), and increases rapidly until  $B_a = 0.0325B_0$  in case (A) and  $B_a = 0.0375B_0$  for (B). The experimental peak position of the Hall resistance  $B_a = 0.04B_0$  is very close to these values. For larger  $B_a$  the curve almost coincides with the one in Fig. 5, which is due to the exponential form of  $t/T$ .

Notice that for case (B) the peak is very close to the experimental position and the qualitative behaviour of the Hall resistance is reproduced, the experimental curve differs quantitatively with the theoretical one only for  $B_a > 0.04B_0$ . Our Hall resistance in this magnetic field range is smaller than measured experimentally. From this comparison it seems that the cycloidlike electron trajectories do not contribute much for large applied magnetic field  $B_a$ . This might be due to a large concentration of scatterers underneath the magnetic stripe edge, which might arise from the fabrication process of the sample. This would not only result in an increase of the resistance, but would especially hamper/kill the cycloidlike states propagating underneath it.

Due to the fact that the Hall resistance for large  $B_a$  equals the two terminal resistance, it is possible to estimate  $\alpha$  by comparison of the theoretical curve with the experimental one. In order to obtain reasonable agreement with the experimental curve, we have to assume  $\alpha = 1.59$ . This value is now fixed and will be used to compare our theoretical results on the magnetoresistance with the experimental results of Ref. 18.

#### V. THE MAGNETORESISTANCE

In order to measure the magnetoresistance, the voltage probes are on the same side of the wire and separated a distance from each other along the 1D wire as shown schematically in Fig 2(b). If the probes are situated on the same side (which is the case for the curves under study), we can approximate the transmission probabilities by:  $T_{31} = T$ ,  $T_{32} = (1 - \beta)t$ ,  $T_{42} = (1 - \beta)T$ ,  $T_{43} = t$ , where  $\beta < 1$  is defined as the fraction of the current  $I_{12}$  which is reflected due to collisions between probe 3 and 4. The magnetoresistance is then given by

$$R_{12,34} = \frac{\hbar}{e^2} \frac{1}{T_{12}} \frac{(2 - \beta)\beta}{\left[\frac{t}{T} + \frac{T}{t}\right](1 - \beta) + \beta^2 - 2\beta + 2}. \quad (12)$$

Note that in this case there are two parameters  $\alpha$  and  $\beta$  and one function  $t/T$  which determine the Hall resistance.

In absence of any magnetic field,  $t/T = 1$  and we obtain for the form factor  $F \approx \beta/(2 - \beta)$ . For increasing magnetic field  $B_a$ ,  $t/T$  will decrease rapidly and for  $B_a \gg 0$ ,  $t/T < 1$ , which results in  $F = (t/T)(2\beta)/(1 - \beta)$ .

Theoretically  $\alpha$  and  $t/T$  are identical to those of the previous section and we have only to determine the parameter  $\beta$ . It is clear that also this parameter depends

on the distance between the two voltage probes, the scattering time and the velocity of the electron states at the Fermi-level. For simplicity we will consider  $\beta(B_a) \approx \beta$  to be independent of the magnetic field, which is justified since the function  $t/T(B_a)$  changes more drastically than  $\beta(B_a)$ . We will show that this approximation already results in good qualitative agreement with the experimental curves.

If we insert  $\alpha = 1.59$  and  $t/T$  identical to the ones obtained from the Hall resistance, we arrive at the magnetoresistance shown in Fig. 7. In this figure we took  $\beta = 0.95$  and plotted  $R_{12,35}$  for case (A) (dotted curve) and case (B) (solid curve) together with the experimental result of Nogaret *et al.* (dashed curve), which is plotted with respect to the right hand axis. We find a peak in the resistance at  $B_a = 0.02B_0$  in case (A), and  $B_a = 0.0275B_0$  for (B). The experimental peak position ( $B_a = 0.03B_0$ ) (dotted curve) is very close to our theoretical result for case (B). Notice that the peak position occurs for smaller  $B_a$  than for the induced Hall resistance, which is in correspondence with the experimental results.

In contrast to the experimental results, we notice that for large  $B_a$ -values the magnetoresistance is zero. This is due to the fact that we have assumed that for large  $B_a$ -values,  $t/T = 0$ . But due to scattering there is always a possibility for an electron to be scattered from an edge state localized on one side of the sample to an edge state on the other side (and traveling in the other direction). If we assume that this effect results in a constant remainder  $t_0 = 0.005$  and corresponding  $t/T = (1 - t_0) \exp[-25B_a - (35B_a)^2] + t_0$ , we obtain the positive magnetoresistance as measured experimentally. This background does not change the Hall resistance qualitatively: the slope decreases, but this can easily be compensated with a larger  $\alpha$  in order to have good agreement with the experiment.

It is very hard to reproduce the experimental results quantitatively, as is obvious from the need for a different left and right axis. The magnitude of the experimental result is larger, and an additional background is present. Due to the approximations made in our simple approach, we underestimated the magnetoresistance. Moreover, the experiment also suffers from other effects, like backscattering etc., which also influence the resistance but which we did not take into account in this paper. Nevertheless, we were able to reproduce the position and the magnitude ( $\approx 150 \Omega$ ) of the peak.

## VI. CONCLUSIONS

In this paper we studied electron transport in a quantum wire subjected to an abrupt magnetic field gradient arising from a ferromagnetic stripe fabricated at its surface, as was investigated experimentally by Nogaret *et al.*<sup>18</sup> We were able to reproduce the main qualita-

tive features of the magnetic field dependence of the Hall and magnetoresistance. In particular, the position of the peak in both resistances was correctly explained. This peak is due to two competing effects, i.e. the increase of the separation between subbands for increasing magnetic field, which decreases the number of conducting channels, and the killing of snake orbits and the creation of states which travel in the opposite direction of ordinary snake orbits, the so called cycloidlike states.<sup>16</sup> Two models for the magnetization of the ferromagnetic stripe were considered corresponding to the extreme cases of a hard (A) and a soft (B) magnet. Model (B) gives the closest agreement with experiment which agrees with the observation by Nogaret *et al.* that almost no hysteresis was observed.

In comparison with the theoretical approach of Nogaret *et al.*,<sup>18</sup> ours differs essentially in two ways: (1) the magnetic field profile is the one created by a soft magnet while Nogaret *et al.* assumed a magnetic barrier which is already present for zero applied magnetic field, and (2) we calculated the Hall and magnetoresistance for a four probe measurement with particular geometry, by use of a semi-classical theory based on the Landauer-Büttiker formula, while Nogaret *et al.*<sup>18</sup> made use of a semi-classical drift diffusion model.

## ACKNOWLEDGMENTS

This work was partially supported by the Interuniversity Micro-Electronics Center (IMEC, Leuven), the Flemish Science Foundation (FWO-VI), the ‘‘Onderzoeksrraad van de Universiteit Antwerpen’’, and the IUAP-IV. J.R. was supported by ‘‘het Vlaams Instituut voor de bevordering van het Wetenschappelijk & Technologisch Onderzoek in de Industrie’’ (IWT) and F. M. P. is a research director with the FWO-VI. We acknowledge fruitful correspondence with A. Nogaret.

---

\* Electronic mail: peeters@uia.ua.ac.be

<sup>1</sup> For a recent overview see: F. M. Peeters and J. De Boeck, in *Handbook of nanostructured materials and nanotechnology*, Edited by H. S. Nalwa, Vol. 3 (Academic Press, New York, 1999), p. 345.

<sup>2</sup> J. de Boeck and G. Borghs, *Physics World* (April, 1999), p. 27.

<sup>3</sup> M. Johnson, B. R. Bennett, M. J. Yang, M. M. Miller, and B. V. Shanabrook, *Appl. Phys. Lett.* **71**, 974 (1997); F. G. Monzon, M. Johnson, and M. L. Roukes, *Appl. Phys. Lett.* **71**, 3087 (1997).

<sup>4</sup> J. Reijniers and F. M. Peeters, *Appl. Phys. Lett.* **73**, 357 (1998); J. Reijniers and F. M. Peeters, *J. Appl. Phys.* **87**, 8088 (2000).

- <sup>5</sup> F. M. Peeters and X. Q. Li, Appl. Phys. Lett. **72**, 572 (1998).
- <sup>6</sup> F. M. Peeters and A. Matulis, Phys. Rev. B **48**, 15166 (1993).
- <sup>7</sup> A. Matulis, F. M. Peeters, and P. Vasilopoulos, Phys. Rev. Lett. **72**, 1518 (1994).
- <sup>8</sup> V. Kubrak, F. Rahman, B. L. Gallagher, P. C. Main, M. Henini, C. H. Marrows, and M. A. Howson, Appl. Phys. Lett. **74**, 2507 (1999).
- <sup>9</sup> T. Vančura, T. Ihn, S. Broderick, K. Ensslin, W. Wegscheider, and M. Bichler, Phys. Rev. B **62**, 5074 (2000).
- <sup>10</sup> M. Kato, A. Endo, M. Sakairi, S. Katsumoto, and Y. Iye, J. Phys. Soc. Jpn. **68**, 2870 (1999).
- <sup>11</sup> A. Matulis and F. M. Peeters, Phys. Rev. B **62**, 91 (2000).
- <sup>12</sup> J. E. Müller, Phys. Rev. Lett. **68**, 358 (1992).
- <sup>13</sup> I. S. Ibrahim and F. M. Peeters, Phys. Rev. B **52**, 17321 (1995).
- <sup>14</sup> S. D. M. Zwerschke, A. Manolescu, and R. R. Gerhardt, Phys. Rev. B **60**, 5536 (1999).
- <sup>15</sup> A. A. Bykov, G. M. Gusev, J. R. Leite, A. K. Bakarov, N. T. Moshegov, M. Cassé, D. K. Maude and J. C. Portal, Phys. Rev. B. **61**, 5505 (2000).
- <sup>16</sup> J. Reijniers and F. M. Peeters, J. Phys.: Condens. Matter (2000).
- <sup>17</sup> B.-Y. Gu, W.-D. Sheng, X.-H. Wang and J. Wang, Phys. Rev. B **56**, 13434 (1997)
- <sup>18</sup> A. Nogaret, S. J. Bending and M. Henini, Phys. Rev. Lett. **84**, 2231 (2000).
- <sup>19</sup> M. Büttiker, Phys. Rev. Lett. **57**, 1761 (1986).
- <sup>20</sup> F. M. Peeters, Phys. Rev. Lett. **61**, 589 (1988).
- <sup>21</sup> F. M. Peeters, Superlattices and Microstructures **6**, 217 (1989).

FIG. 1. The top (a) and side view (b) of the sample configuration used by Nogaret *et al.*<sup>18</sup> In (c) the resulting (modeled) magnetic field profile in the wire is shown with  $B_i$  the magnetic field profile due to the fringe fields and  $B_a$  the uniform externally applied field.

FIG. 2. Four-terminal configuration in (a) a Hall and (b) a magnetoresistance measurement. In a magnetic field the electron current flows along the edge. This current is schematically shown together with the different transmission probabilities.

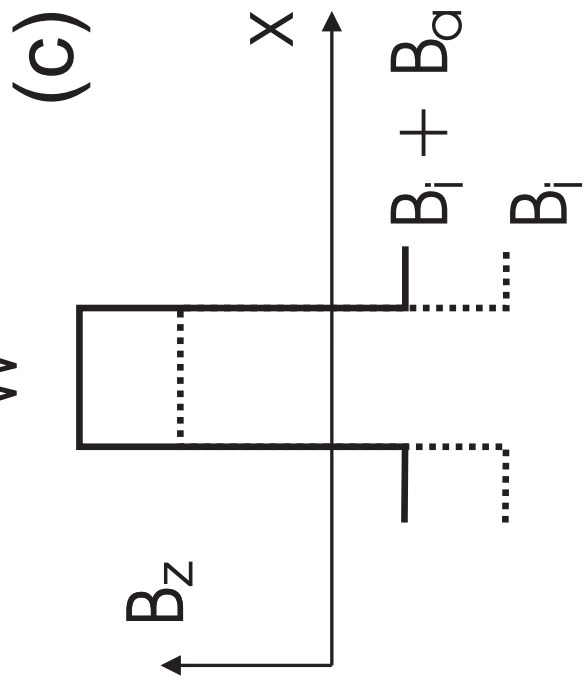
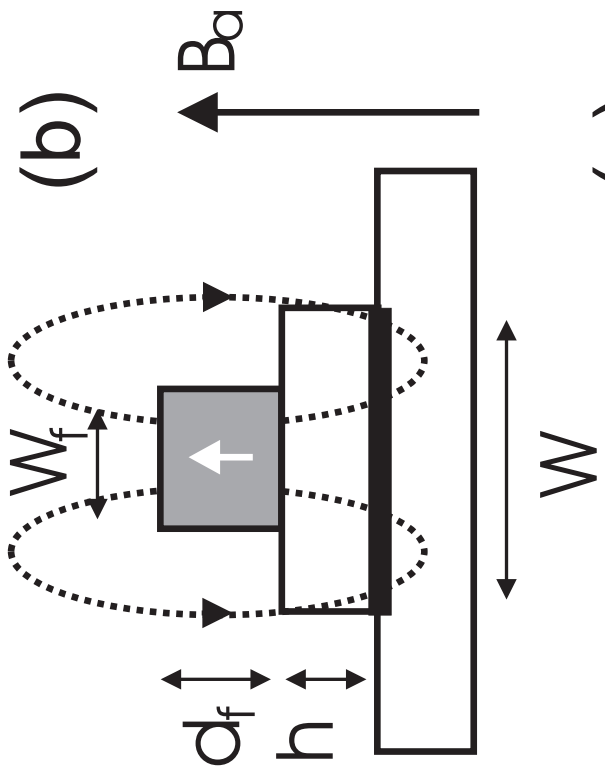
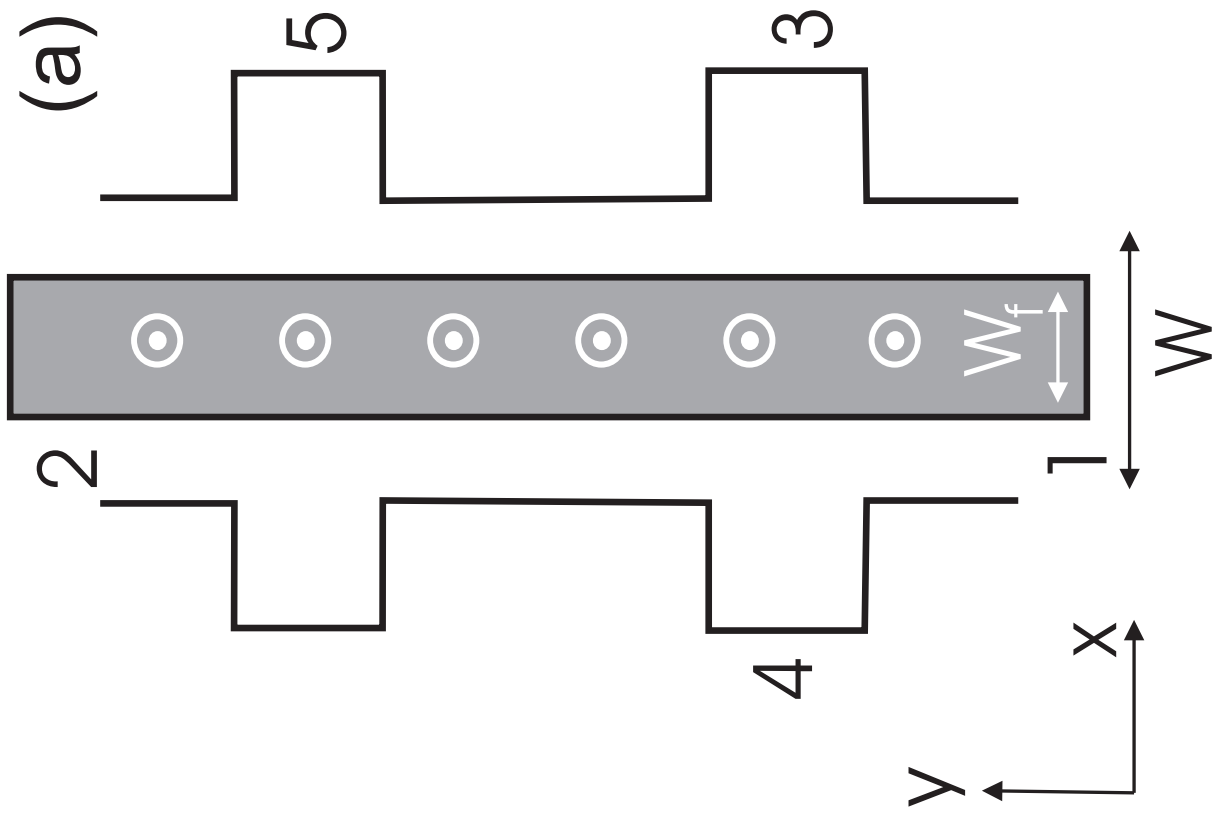
FIG. 3. The energy spectrum in case (A) as function of  $k$  for (a)  $B_a/B_0 = 0$ , (b) 0.1, and (c) 0.5. The classical trajectories for  $\epsilon_F = 4E_0$  are schematically shown on top of the figures for the  $k$ -range indicated by the solid bars. The darker area in these insets correspond to the position of the magnetic stripe.

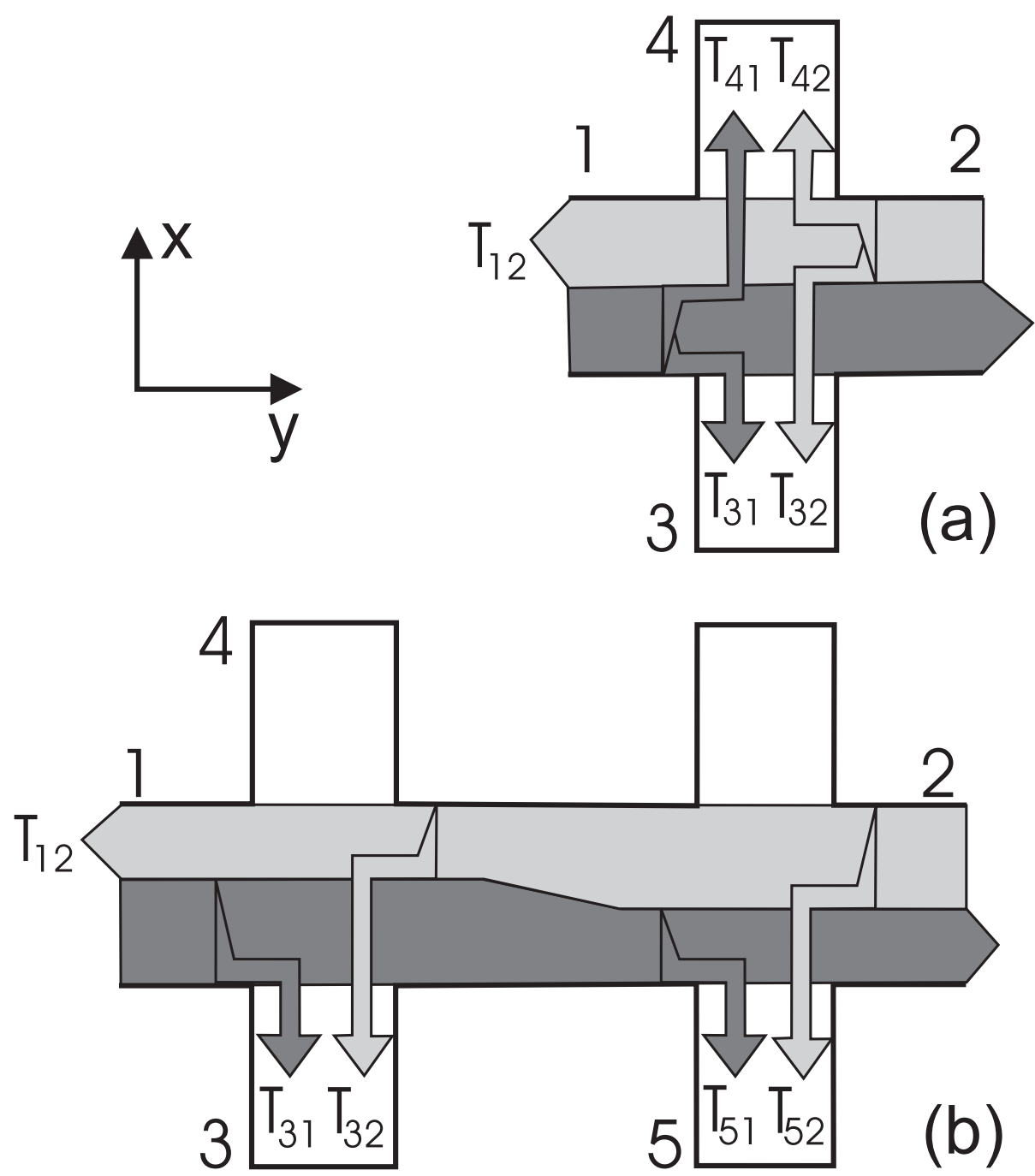
FIG. 4. The same as in Fig. 3, but now for case (B) for (a)  $B_a/B_0 = 0$ , (b) 0.03 and (c) 0.06.

FIG. 5. The induced two point resistance  $R_{12,12}/R_{12,12}^0$  as function of  $B_a$  for case (A) (dotted curve) and case (B) (solid curve), and according to the approach of Nogaret *et al.* (dashed curve). The inset shows the zero temperature induced resistance.

FIG. 6. The induced Hall resistance  $R_{12,34}/R_{12,34}^0$  as function of the applied magnetic field  $B_a$  as measured experimentally by Nogaret *et al.* (dashed curve) and our theoretical result for case (A) (dotted curve) and case (B) (solid curve).

FIG. 7. The magnetoresistance  $R_{12,35}$  as function of the applied magnetic field  $B_a$  in case (A) (dotted curve) and (B) (solid curve). The latter is plotted with and without remainder  $t_0$ . The experimental result of Nogaret *et al.* (dashed curve) is plotted with respect to the axis on the right hand side





This figure "fig3large.jpg" is available in "jpg" format from:

<http://arxiv.org/ps/cond-mat/0009303v1>

This figure "fig4large.jpg" is available in "jpg" format from:

<http://arxiv.org/ps/cond-mat/0009303v1>

